




## ENTROPY GENERATION OPTIMIZATION IN A REE-EYRING TERNARY HYBRID NANOFLUID FLOW OVER AN ELASTIC SURFACE WITH NON-FOURIER HEAT FLUX

 **Gadamsetty Revathi**<sup>a</sup>,  **D. Purnachandra Rao**<sup>b</sup>,  **S. Ramalingeswara Rao**<sup>c</sup>,  **K.S. Srinivasa Babu**<sup>c\*</sup>,  
 **T.R.K.D. Vara Prasad**<sup>c</sup>,  **M. Jayachandra Babu**<sup>d</sup>

<sup>a</sup>Department of Mathematics, Gokaraju Rangaraju Institute of Engineering and Technology, Bachupally, Hyderabad – 500090, India

<sup>b</sup>Department of Mathematics, Matrusri Engineering College, Saidabad, Hyderabad – 500059, Telangana, India

<sup>c</sup>Department of EM&H, S.R.K.R. Engineering College, Bhimavaram, Andhra Pradesh – 534204, India

<sup>d</sup>Department of Mathematics, Government Degree College, Rajampeta, Annamayya district, Andhra Pradesh – 516115, India

\*Corresponding Author e-mail: [kssb@srkrec.ac.in](mailto:kssb@srkrec.ac.in)

Received September 14, 2024; revised November 12, 2024; accepted November 20, 2024

The significance of Ree-Eyring ternary hybrid nanofluid flow lies in its potential applications in various fields. By incorporating three different types of nanoparticles into a base fluid using the Ree-Eyring model, this innovative fluid offers enhanced thermal conductivity, heat transfer efficiency, and rheological properties. These characteristics are particularly valuable in industries such as electronics cooling, solar energy systems, and heat exchangers, where efficient heat management is crucial. Additionally, the unique rheological behavior of Ree-Eyring nanofluids can provide advantages in processes like drilling, lubrication, and drug delivery. Under Thompson-Troian boundary conditions, this study aims to theoretically analyse 2D radiative flow of the Ree-Eyring ternary hybrid nanofluid over an angled sheet with Cattaneo-Christov heat flux and higher order chemical reaction parameters. In order to express them as ordinary differential equations (ODEs), flow-driven equations undergo suitable similarity transformations. The ensuing system is resolved by employing a bvp4c approach. The main takeaway from this study is that the thermal relaxation parameter reduces the width of the temperature profile and the fluid velocity is minimized by adjusting the slip parameter. The concentration profile is minimized by the chemical reaction parameter and the Ree-Eyring fluid parameter increases with the same (fluid velocity). In addition, we found that the skin friction coefficient is strongly correlated negatively with the Ree-Eyring fluid parameter, positively with the (thermal) relaxation parameter, and significantly correlated positively with the chemical reaction through the Nusselt number. When Brinkman number increases, Bejan number drops. Furthermore, a rise in thermal radiation parameter leads to the escalation in both entropy generation and Bejan number. We observed a worthy agreement when we checked the outcomes of this investigation with prior effects.

**Keywords:** Viscous dissipation; Thermal Radiation; MHD; Non-Fourier Heat Flux; Nanofluid

**PACS:** 47.15.-x, 47.50.-d

### Nomenclature

$u, v$  – Components of velocity in  $x, y$  directions respectively  
 $\rho$  – Fluid density  
 $\mu$  – Dynamic viscosity  
 $g$  – Acceleration due to gravity  
 $\alpha$  – Angle of inclination  
 $\nu_w$  – Permeability of porous surface  
 $\sigma$  – Electric conductivity  
 $T$  – Fluid temperature (dimensional)  
 $\xi^*$  – Critical shear rate  
 $\beta, c$  – fluid constants  
 $\beta_T$  – Thermal expansion coefficient  
 $\beta_C$  – Concentration expansion coefficient  
 $C_p$  – Specific heat capacity  
 $k_0$  – Chemical reaction parameter  
 $B_0$  – Initial magnetic strength  
 $M$  – Magnetic field parameter

$\gamma^*$  – Navier's slip length  
 $\nu$  – Kinematic viscosity  
 $C$  – Fluid concentration (dimensional)  
 $k^*$  – Mean absorption coefficient  
 $\sigma^*$  – Stefan-Boltzmann constant  
 $D_m$  – Molecular diffusivity  
 $\Lambda$  – Thermal relaxation parameter  
 $Sc$  – Schmidt number  
 $We$  – Ree-Eyring fluid parameter  
 $\lambda_1$  – Mixed convection parameter  
 $\lambda_1^*$  – Buoyancy ratio parameter  
 $R_a$  – Radiation parameter  
 $E_c$  – Eckert number  
 $Bn$  – Bejan number  
 $Br$  – Brinkman number  
 $\theta$  – Fluid temperature (non-dimensional)  
 $\phi$  – Fluid concentration (non-dimensional)

### 1. INTRODUCTION

Nanofluids are the colloidal mixtures of ordinary liquid particles having a dimension of less than one nanometre. These particles will enhance the thermal properties of typical liquids with low thermal conductivity. The latest generations have used a number of innovative techniques to increase the heat transfer rates, which has allowed them to achieve different degrees of thermal adeptness. Enhancing heat conduction is necessary to do this. Thus, many attempts were made to increase heat conductivity in the liquids by dispersing higher, solid thermally conductive components throughout them. The goal of developing nanofluids to meet industrial demands has been attempted multiple times. While efforts to develop a superior fluid are still on, researchers and experts in energy use might discover that nanofluids meet their

requirements. For instance, Sheikholeslami and Rokni [1] has been studied the behaviour of heat transfer of a nanofluid along with magnetic effect. Ganvir et al. [2] discussed the characteristics of transmission of heat in a nanofluid. Revathi et al. [3] conducted research on the flow of Darcy–Forchheimer power-law (Ostwald-de Waele type) nanofluid past an inclined plate subject to the influences of thermal radiation, activation energy. Recently, Rasool et al. [4] reported the results for the MHD radiative Darcy-Forchheimer nanofluid flow. Along a porous rotating disk, a stagnant Maxwell nanofluid flow and heat transfer is another study of Li et al. [5]. Radiative motion of a Water- $\text{Al}_2\text{O}_3$  based nanofluid past a Riga surface with thermal radiation is reported by Madhukesh et al. [6]. Modelling of nanofluids with a mixture of two or more special types of nanoparticles treating as hybrid as well as ternary hybrid nanofluids based on their greater heat transfer production is another interesting aspect in the present literature. Huge amount of research can be observed from the recent literature on it. For instance, Yasir et al. [7] conducted research on a mixed convective radiative Hybrid nanofluid with heat generation/absorption impacts. Kho et al. [8] discussed the impacts of viscous dissipation and thermal radiation in a MHD flow of hybrid nanofluid. Abbas et al. [9] presented the numerical findings on a convective motion of a hybrid nanofluid along an infinite disk. Focusing on the very recent articles Khan et al. [10], Mishra and Pathak [11], Najafpour et al. [12], Farooq et al. [13], Mahboobtosi et al. [14] and Mohanty et al. [15], one can notice the similar attempts which are noteworthy.

The Cattaneo-Christov heat flux model is a mathematical approach, which can be utilized to describe transfer of heat in fluids and materials. It represents an improvement over the classical Fourier's law on conduction of heat. In contrast to the instantaneous heat transmission assumed by Fourier's law, the Cattaneo-Christov model includes a thermal relaxation time. This time constant reflects the finite time it takes for a material's temperature to adjust to a change in heat flux. This is particularly important for studying heat transfer at the microscopic level or in situations with rapid temperature variations. The model is used to analyze heat transfer in boundary layer flows, where thin layers of fluid develop near surfaces with different temperatures. This is applicable in various engineering contexts like heat ex-changers and fluid flow over objects. Most relevant applications of said model particularly occurs in engineering and biomedical processes. Metal spinning, nuclear reactor cooling, magnetic drug targeting, hot rolling, drawing copper wires, heat conduction in tissues and in energy production etc. Hayat et al. [16] included Cattaneo-Christov (C-C) mass flux model to scrutinize the features of heat transmission in the investigation of non-Newtonian fluid flow. Ahmad et al. [17] considered a wedge and numerically examined micropolar fluid flow by using *bvp4c* technique in MATLAB with thermal relaxation time and observed that it alleviates fluid temperature. Ibrahim and Gadisa [18] considered CCHF and examined the Oldroyd-B fluid flow by an irregular elongating sheet. They emphasized that this fluid model is good at examining the dilute polymeric solutions for visco-elastic behaviour. Reddy et al. [19] and Gireesha et al. [20] discussed various dusty fluid flows by a stretching sheet with CCHF model. They identified the fact that radiation parameter is predominant in cooling procedure and observed that the melting parameter lessens fluid temperature. Ali et al. [21] applied variational FEM (finite element method) to unriddle the mathematical model in the rotational Casson fluid flow examination through an extendable surface with double diffusive Cattaneo-Christov and detected diminution in secondary velocity with larger magnetic field parameter. Tassaddiq [22] considered elastic body and elucidated a micropolar-hybrid fluid flow with CCHF and Ohmic heating. Jakeer et al. [23] identified that the larger Darcy number ameliorates the fluid velocity in the scrutiny of HNF within a porous cavity with CCHF model. Examination of HNF (water with graphene and silver) flow among rotating disks with CCHF is done by Mahesh et al. [24] and amelioration in tangential velocity with larger Reynolds number is one of their results. Ali et al. [25] utilized Galerkin technique to theoretically examine the rotational nanofluid flow by an elastic surface and discovered that the Lewis number escalates the value of Sherwood number. Recently, several authors [26-33] considered various geometries and scrutinised diverse fluid flows with CCHF model.

Surface stretching mechanism in flow dynamical problems has become widely accepted in many industrial and technological processes. In particular, the quantity and quality of industrial processes heavily rely on the stretching of sheets. Rubber sheeting, hot rolling, glass blowing, drawing of wires, manufacturing of glass, processes like polymerization of sheets are some of the usages of stretching mechanisms. By using numerical simulations, Khan et al. [34] were able to observe that the Soret effect improves the concentration profile when MHD nanofluid flows through an extending sheet. Activation energy included Nanofluid flow was studied by Rasool et al. [35], who found that it reduces the mass flux rate. Abbas et al. [36] applied HAM method to elucidate MHD flow of Carreau fluid with varying thermal conductivity. Yasmin et al. [37] examined the features of heat transfer in the flow of MHD micropolar fluid by a tilted stretchable surface and detected that fluid velocity is minified with larger curvature parameter. Sankar Giri et al. [38] considered stretching cylinder and scrutinized MHD nanofluid (CNT nanoparticles) flow with chemical reaction. Gayatri et al. [39] considered nonuniform elongating sheet and discussed MHD dissipative Carreau fluid flow with Ohmic heating. Kumar et al. [40] used FEM to unriddle the mathematical model in their study on MHD fluid flows with various spherical nanoparticles by a vertical plate and noticed an inverse relationship among magnetic field parameter and Nusselt number. Newly, several researchers [41-52] discussed various MHD fluid flows through a variety of stretchable geometries.

Upon reviewing the aforementioned literature, it became apparent that the Ree-Eyring ternary hybrid nanofluid flow across an angled stretchable sheet subjected to Thompson-Troian boundary conditions has not been previously investigated. The originality of this study is in its examination of the dissipative magnetohydrodynamic Ree-Eyring ternary hybrid nanofluid flow via an angled plate with boundary conditions imposed by Thompson Troian theory. Entropy

optimization and Bejan number calculation were also included in this study. Two events, suction and injection, are depicted graphically to show the consequences. Findings of this study are well agreed with already published results which was shown in validation section.

### 2. FORMULATION

A radiative and chemically reactive motion of a Ree-Eyring ternary hybrid nanofluid across an elastic surface (angled) in addition to Thompson-Troian boundary conditions is investigated theoretically in the present analysis. The following hypotheses form the basis of the current inquiry:

- (i) The utilisation of non-Fourier heat flux is aptly applied in the examination of thermal conduction processes.
- (ii) kindly see Table 1 for exact numerical calculations of the thermo-physical properties of water ( $H_2O$ ), Graphene,  $SiO_2$ , and  $CuO$ .
- (iii) Sheet is inclined by an angle  $\alpha$  (observe Fig. 1).
- (iv) An external magnetic field applied vertically with an intensity  $B_0$  influences the flow.
- (v) In this work, the influence of induced magnetic fields is ignored.

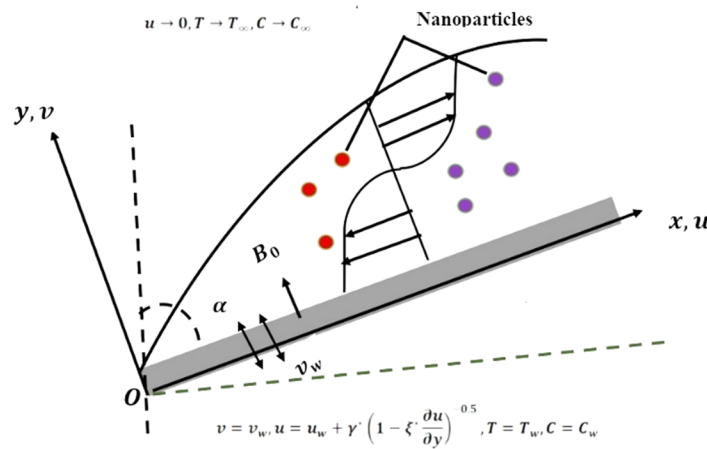


Figure 1 Schematic representation of the present situation

Table 1. Key parameters' values of  $H_2O$ , Graphene,  $SiO_2$ , and  $CuO$

S. No.	Properties	$H_2O$ ( $f$ )	Graphene ( $\Phi_G$ )	$SiO_2$ ( $\Phi_S$ )	$CuO$ ( $\Phi_C$ )
1	$\sigma(S/m)$	0.005	$10^7$	$10^{-25}$	$2.7 \times 10^{-8}$
2	$k(W/mK)$	0.613	2500	1.38	76.5
3	$\rho(Kg/m^3)$	997.1	2250	2200	6320
4	$C_p(J/KgK)$	4179	2100	703	531.8

Here are the conditions (prerequisites) and basic equations required for the study, based on these presumptions:

$$\frac{\partial u}{\partial x} + \frac{\partial v}{\partial y} = 0, \tag{1}$$

$$v \frac{\partial u}{\partial y} + u \frac{\partial u}{\partial x} = \rho_{thnf}^{-1} \left( \mu_{thnf} + \frac{1}{\beta c} \right) \left( 2 \frac{\partial^2 u}{\partial x^2} + \frac{\partial^2 v}{\partial x \partial y} + \frac{\partial^2 u}{\partial y^2} \right) + \beta_c (C - C_\infty) g \cos \alpha, \tag{2}$$

$$+ \beta_T (T - T_\infty) g \cos \alpha - \rho_{thnf}^{-1} \sigma_{thnf} u B_0^2$$

$$u \frac{\partial T}{\partial x} + v \frac{\partial T}{\partial y} = k_{thnf} (\rho C_p)_{thnf}^{-1} \frac{\partial}{\partial y} \left( \frac{\partial T}{\partial y} \right) + (\rho C_p)_{thnf}^{-1} \frac{4 T_\infty^3 \sigma^*}{3 k^*} \frac{\partial}{\partial y} \left( \frac{\partial T}{\partial y} \right) \tag{3}$$

$$- \gamma \left[ \left( u \frac{\partial v}{\partial x} + v \frac{\partial v}{\partial y} \right) \frac{\partial T}{\partial y} + v^2 \frac{\partial^2 T}{\partial y^2} + 2uv \frac{\partial^2 T}{\partial x \partial y} + u^2 \frac{\partial^2 T}{\partial x^2} \right] + (\rho C_p)_{thnf}^{-1} \left( \mu_{thnf} + \frac{1}{\beta c} \right) \left( \frac{\partial u}{\partial y} \right)^2,$$

$$u \frac{\partial C}{\partial x} + v \frac{\partial C}{\partial y} = \frac{\partial^2 C}{\partial y^2} D_m - (C - C_\infty)^m k_0, \tag{4}$$

$$\left. \begin{aligned} \text{at } y = 0 : v = v_w, u = u_w + u_f = bx + \gamma^* (1 - \xi^* u_y)^{-0.5} \frac{\partial u}{\partial y} \Big|_{y=0}, T = T_w, C = C_w, \\ \text{as } y \rightarrow \infty : u \rightarrow 0, T \rightarrow T_\infty, C \rightarrow C_\infty. \end{aligned} \right\} \text{(Ahmad and Nadeem [53])} \tag{5}$$

The following similarity transmutations for transforming controlling equations were offered by Rafique et al. [54]:

$$\left. \begin{aligned} \theta = \frac{T - T_\infty}{T_w - T_\infty}, u = bx \frac{df}{d\eta} = bxf'(\eta), v = -f(bv)^{0.5}, \\ C = C_\infty + \phi(\eta)(C_w - C_\infty), \eta = \sqrt{\frac{b}{v}}y. \end{aligned} \right\} \tag{6}$$

Through the use of (6), the continuity equation (1) is satisfied in a straightforward manner. Then (6) was skilfully used to alter (2, 3, 4 and 5) in the following procedure:

$$\frac{1}{S_1} \left( \frac{1}{S_2} + We \right) f''' + ff'' - f'^2 - \frac{S_3}{S_1} Mf' + \lambda_1 (\theta + \phi \lambda_1^*) \cos \alpha = 0 \tag{7}$$

$$\frac{(S_4 + R_a)}{S_5 \text{Pr}} \theta'' + \left[ f\theta' - (ff'\theta' + f^2\theta'') \Lambda + \frac{1}{S_2 S_5} E_c (We + 1) f'^2 \right] \text{Pr} = 0 \tag{8}$$

$$\frac{1}{Sc} \phi'' - \Gamma \phi^m + f\phi' = 0 \tag{9}$$

$$\left. \begin{aligned} \text{at } \eta = 0 : f(\eta) = S, f'(\eta) = 1 + \delta(1 - f''(\eta)\xi)^{-0.5} f''(\eta), \theta(\eta) = \phi(\eta) = 1, \\ \text{as } \eta \rightarrow \infty : f'(\eta) \rightarrow 0, \theta(\eta) \rightarrow 0, \phi(\eta) \rightarrow 0. \end{aligned} \right\} \tag{10}$$

Here

$$\left. \begin{aligned} \lambda_1 = \frac{Gr}{\text{Re}_x^2}, S = -\frac{v_w}{\sqrt{bv}}, E_c = \frac{u_w^2}{C_p(T_w - T_\infty)}, \lambda_1^* = \frac{Gc}{Gr}, \delta = \gamma^* \sqrt{\frac{b}{v}}, \xi = b \sqrt{\frac{b}{v}} \xi^* x, \\ \text{Pr} = \frac{\mu C_p}{k}, M = \frac{B_0 \sigma}{b\rho}, \Lambda = \gamma b, We = \frac{1}{\mu\beta c}, R_a = \frac{16 \sigma^* T_\infty^3}{3 k k_\infty}, Gr = \frac{gx^3 \beta_T (T_w - T_\infty)}{v^2}, \\ Sc = \frac{v}{D_m}, Gc = \frac{gx^3 \beta_C (C_w - C_\infty)}{v^2}, \Gamma = \frac{k_0 (C_w - C_\infty)^{m-1}}{b}, \text{Re}_x = \frac{xu_w}{v}. \end{aligned} \right\}$$

and

$$\left. \begin{aligned} S_1 = (1 - \Phi_G) \left\{ (1 - \Phi_S) \left[ (1 - \Phi_C) + \Phi_C \frac{\rho_C}{\rho_f} \right] + \Phi_S \frac{\rho_S}{\rho_f} \right\} + \Phi_G \frac{\rho_G}{\rho_f}, S_{411} = \frac{k_C + 2k_f - 2\Phi_C(k_f - k_C)}{k_C + 2k_f + \Phi_C(k_f - k_C)}, \\ S_2 = (1 - \Phi_G)^{2.5} (1 - \Phi_S)^{2.5} (1 - \Phi_C)^{2.5}, \sigma_{311} = \frac{\sigma_C - 2(\sigma_f - \sigma_C)\Phi_C + 2\sigma_f}{\sigma_C + (\sigma_f - \sigma_C)\Phi_C + 2\sigma_f}, \\ S_{41} = \frac{k_S + 2S_{411}k_f - 2\Phi_S(S_{411}k_f - k_S)}{k_S + 2S_{411}k_f + \Phi_S(S_{411}k_f - k_S)}, \sigma_{31} = \frac{\sigma_S + 2S_{311}\sigma_f - 2\Phi_S(S_{311}\sigma_f - \sigma_S)}{\sigma_S + 2S_{311}\sigma_f + \Phi_S(S_{311}\sigma_f - \sigma_S)}, \\ S_5 = (1 - \Phi_G) \left\{ (1 - \Phi_S) \left[ (1 - \Phi_C) + \Phi_C \frac{(\rho C_p)_C}{(\rho C_p)_f} \right] + \Phi_S \frac{(\rho C_p)_S}{(\rho C_p)_f} \right\} + \Phi_G \frac{(\rho C_p)_G}{(\rho C_p)_f}, \\ S_4 = \frac{k_G + 2S_{41}k_f - 2\Phi_G(S_{41}k_f - k_G)}{k_G + 2S_{41}k_f + \Phi_G(S_{41}k_f - k_G)}, \sigma_3 = \frac{\sigma_G + 2S_{31}\sigma_f - 2\Phi_G(S_{31}\sigma_f - \sigma_G)}{\sigma_G + 2S_{31}\sigma_f + \Phi_G(S_{31}\sigma_f - \sigma_G)}. \end{aligned} \right\}$$

Friction factor, Nusselt and Sherwood numbers are outlined as:

$$C_{f_x} = \left. \left( \frac{\mu_{thf} + \frac{1}{\beta c}}{\frac{1}{2} \rho u_w^2} \right) \left( \frac{\partial u}{\partial y} + \frac{\partial v}{\partial x} \right) \right|_{y=0}, Nu_x = -x \left. \left( \frac{k_{thf} + \frac{16 \sigma^* T_\infty^3}{3 k^*}}{k_f (T_w - T_\infty)} \right) \frac{\partial T}{\partial y} \right|_{y=0}, Sh_x = -x \left. \frac{D_m}{D_m (C_w - C_\infty)} \frac{\partial C}{\partial y} \right|_{y=0}. \quad (11)$$

Equation (6) allows us to rewrite (11) as

$$(\text{Re}_x)^{0.5} C_{f_x} = 2 \left( \frac{1}{S_2} + We \right) f''(\eta) \Big|_{\eta=0}, (\text{Re}_x)^{-0.5} Nu_x = -(S_4 + R_a) \theta'(\eta) \Big|_{\eta=0}, (\text{Re}_x)^{-0.5} Sh_x = -\phi'(\eta) \Big|_{\eta=0}.$$

### 2.1. Entropy generation and Bejan number

The formula below constitutes the dimensional representation used to calculate the entropy generation in the current work:

$$S_g = \left( \frac{k_{thf} + \frac{16 \sigma^* T_\infty^3}{3 k_f k^*}}{k_f} \right) \frac{k_f}{T_\infty^2} \left( \frac{\partial T}{\partial y} \right)^2 + \frac{1}{T_\infty} \left( \frac{\partial u}{\partial y} \right)^2 \mu_{thf} + \frac{1}{T_\infty} u^2 \sigma_{thf} B_0^2 + \frac{\tilde{R} D_m}{C_\infty} \left( \frac{\partial C}{\partial y} \right)^2 + \frac{\tilde{R} D_m}{T_\infty} \frac{\partial C}{\partial y} \frac{\partial T}{\partial y}. \quad (12)$$

By applying (6), equation (12) can be rewritten as follows:

$$EG = (S_4 + R_a) \alpha \theta'^2 + \frac{1}{S_2} Br f''^2 + S_3 M Br f'^2 + J \frac{\beta_1}{\alpha} \phi'^2 + J \phi' \theta', \quad (13)$$

where:

$$\left. \begin{aligned} EG &= \frac{v T_\infty S_g}{b (T_w - T_\infty) k_\infty}, Br = \frac{\mu u_w^2}{(T_w - T_\infty) k_\infty}, J = \frac{\bar{R} (C_w - C_\infty) D_m}{k_f}, \\ \beta_1 &= \frac{C_w - C_\infty}{C_\infty}, \alpha = \frac{T_w - T_\infty}{T_\infty}. \end{aligned} \right\}$$

The mathematical expression to find the Bejan number is:

$$Bn = \frac{\text{Entropy formation due to the transfer of mass and heat}}{\text{The overall generation of entropy}}.$$

$Bn$  can be restated in the following way by using (13):

$$Bn = \frac{(S_4 + R_a) \alpha \theta'^2 + J \frac{\beta_1}{\alpha} \phi'^2 + J \phi' \theta'}{(S_4 + R_a) \alpha \theta'^2 + \frac{1}{S_2} Br f''^2 + S_3 M Br f'^2 + J \frac{\beta_1}{\alpha} \phi'^2 + J \phi' \theta'}.$$

### 3. VALIDATION

We verified our results with previous results under specific conditions (e.g.,  $We = 0$ ) and found a satisfactory agreement (see Table 2).

**Table 2.** Consistency with prior findings for  $f''(0)$  and  $-\theta'(0)$  to validate our findings

$M$	$f''(0)$		$-\theta'(0)$	
	Devi and Kumar [55]	Current result	Devi and Kumar [55]	Current result
0	-0.5608	-0.56081123	1.0873	1.08733452
0.1	-0.5659	-0.56590213	1.0863	1.08633192
0.2	-0.5810	-0.58101087	1.0833	1.08337829
0.5	-0.6830	-0.68300657	1.0630	1.06300176
1	-1.0000	-1.00000000	1	1
2	-1.8968	-1.89687214	0.8311	0.83118274
5	-4.9155	-4.91554536	0.4703	0.47030201

**4. RESULTS AND DISCUSSION**

Equations (7-9) along with (10) are puzzled out with the bvp4c solver. In this study, solutions are rendered for suction and injection cases.

**4.1. Velocity profile**

As displayed in Fig. 2, the fluid velocity declines as  $M$  upsurges. The Lorentz force grows in amplitude in proportion to the strength of the magnetic field. It leads to a greater reduction in the fluid's velocity. The increment in the Ree-Eyring fluid parameter corresponds to a decrement in the fluid's effective viscosity at higher shear rates. This reduction in viscosity lowers the resistance to flow, allowing the fluid to move more freely and resulting in an increase in fluid velocity [see Fig. 3]. The rise in the volume fraction of nanoparticles in a fluid causes to a rise in viscosity, enhanced inertia, increased drag, and potential microstructure formation. These factors collectively increase the resistance to flow, thereby reducing the overall velocity of the fluid [see Fig. 4].

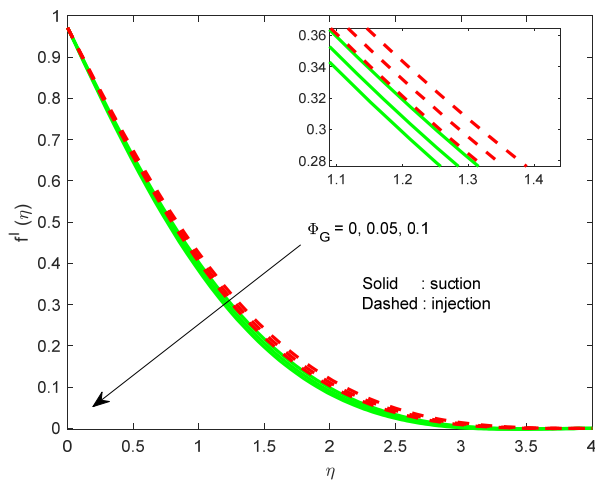


Figure 2. Situation in which  $f'(\eta)$  is impacted by  $\phi_G$

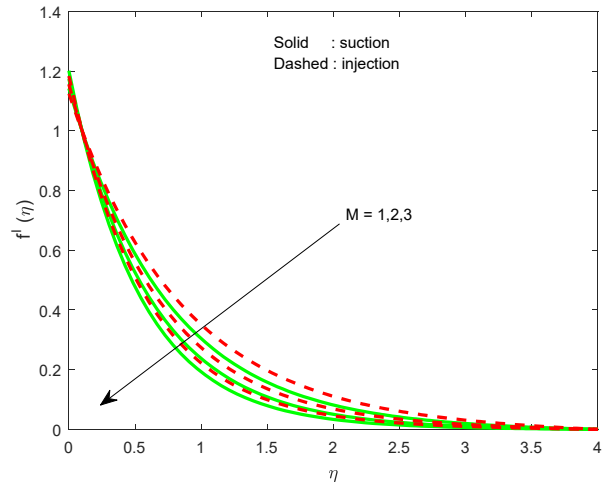


Figure 3. Situation in which  $f'(\eta)$  is impacted by  $M$

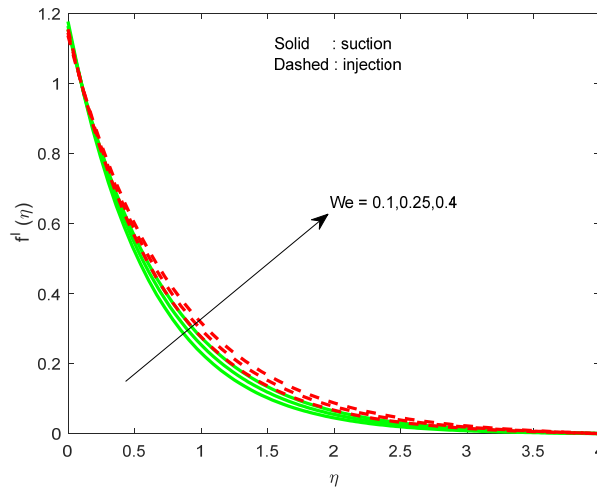


Figure 4. Situation in which  $f'(\eta)$  is impacted by  $We$

**4.2. Temperature profile**

A rise in the Eckert number corresponds to a hike in the relative importance of kinetic energy compared to thermal energy. This results in more kinetic energy being converted into heat through viscous dissipation, causes to a rise in the fluid's temperature [see Fig. 5]. A rise in the thermal relaxation parameter causes the fluid to respond more slowly to thermal disturbances, reducing the rate of heat conduction and energy dispersal within the fluid. As a result, there is a reduction in temperature [see Fig. 6]. An increase in the thermal radiation parameter enhances the amount of radiant energy absorbed by the fluid. This absorbed energy raises the internal energy of the fluid, resulting in a higher temperature [see Fig. 7]. The effect is particularly significant in systems where thermal radiation plays a major role in the heat transfer process, such as in high-temperature applications or in fluids with strong radiative properties.

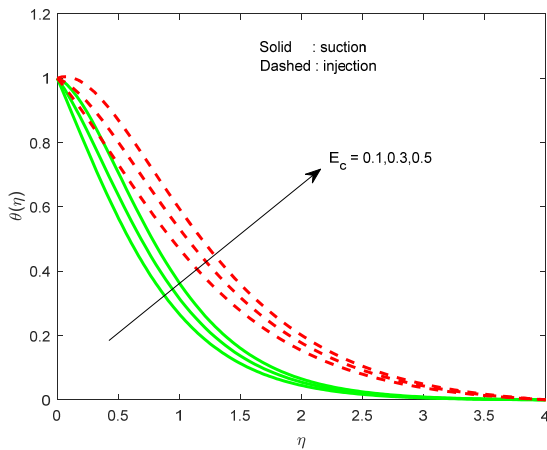


Figure 5. Situation in which  $\theta(\eta)$  is impacted by  $E_c$

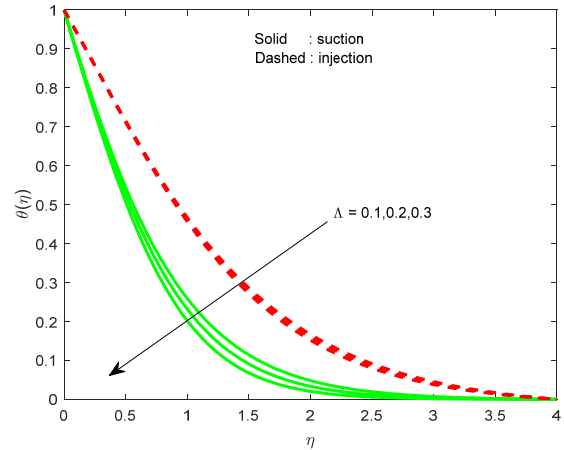


Figure 6. Situation in which  $\theta(\eta)$  is impacted by  $\Lambda$

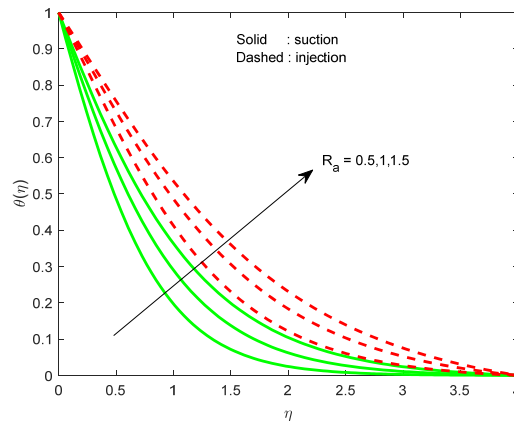


Figure 7. Situation in which  $\theta(\eta)$  is impacted by  $R_a$

### 4.3. Concentration profile

Raising the value of  $Sc$  causes the fluid's concentration to decline, as can be seen in Fig. 8. An increment in the parameter of chemical reaction accelerates the rate at which reactants are altered into products. This heightened reaction rate leads to a more rapid depletion of the reactants, thereby reducing their concentration in the fluid. The balance between mass transfer and chemical reaction shifts towards greater consumption, resulting in a lower overall concentration of the reactant species in the fluid (see Fig. 9).

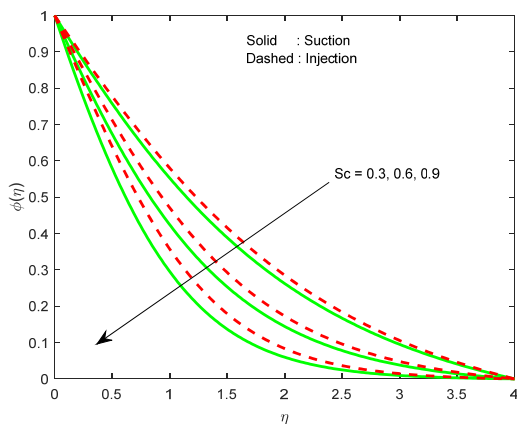


Figure 8. Situation in which  $\phi(\eta)$  is impacted by  $Sc$

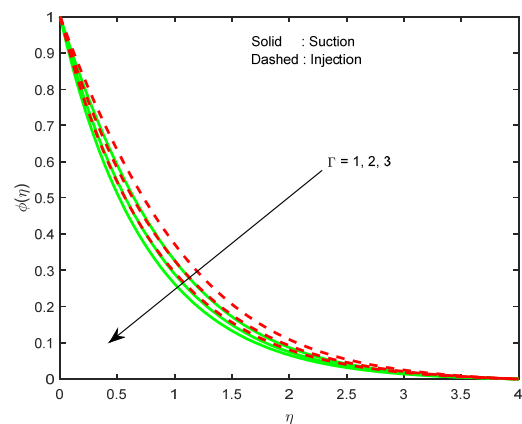
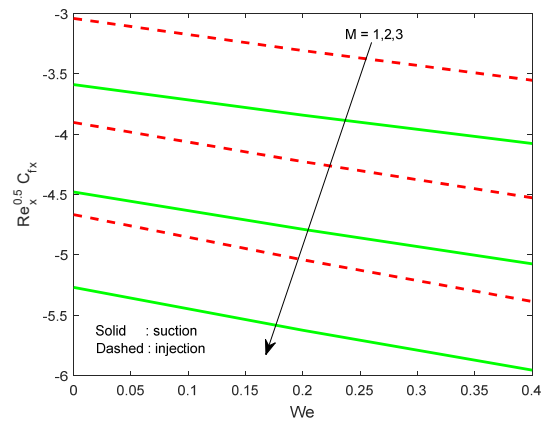
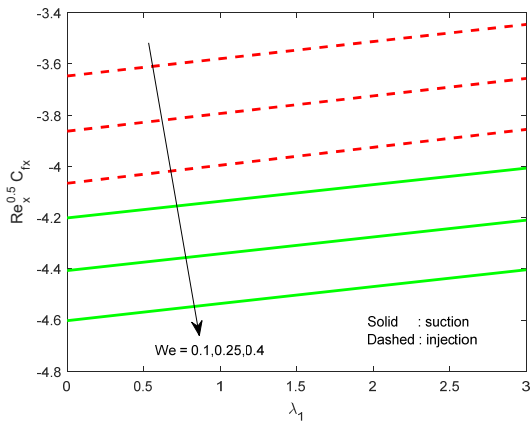


Figure 9. Situation in which  $\phi(\eta)$  is impacted by  $\Gamma$

### 4.4. Engineering quantities of interest

Figs. 10-15 explains the impression of pertinent parameters on heat transmission rate, surface friction drag and mass transmission rate.



**Figure 10.** Situation in which friction factor is impacted by  $We$  **Figure 11.** Situation in which friction factor is impacted by  $M$

It is detected that both Ree-Eyring fluid parameter, magnetic field parameters minimize the surface friction drag (Fig. 10-11). As the Ree-Eyring fluid parameter increases, the fluid exhibits more pronounced shear-thinning behaviour, leading to a reduction in viscosity near the wall where shear rates are high. This reduction in viscosity lowers the wall shear stress, which directly reduces the skin friction coefficient. An increase in the Eckert number enhances viscous dissipation in the fluid, which generates additional heat and reduces the temperature gradient between the heated surface and the fluid. This reduction in the temperature gradient weakens the convective heat transfer, leading to a lower Nusselt number. In essence, the higher the Eckert number, the less efficient the heat transfer becomes, resulting in a reduced Nusselt number (Fig. 12). Rise in thermal relaxation parameter enhances the heat transmission rate as seen in Fig. 13. Furthermore, it is seen that chemical reaction and Schmidt numbers are cooperative to improve mass transmission rate of the fluid (Figs. 14-15).

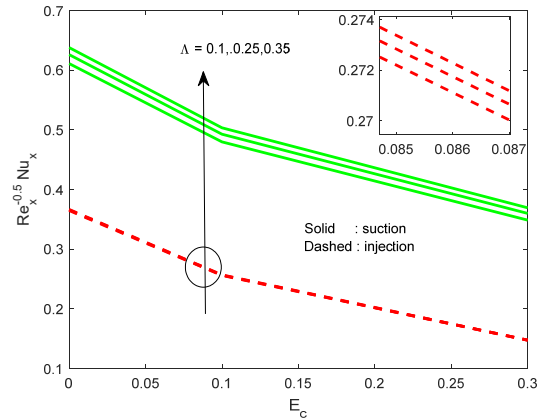
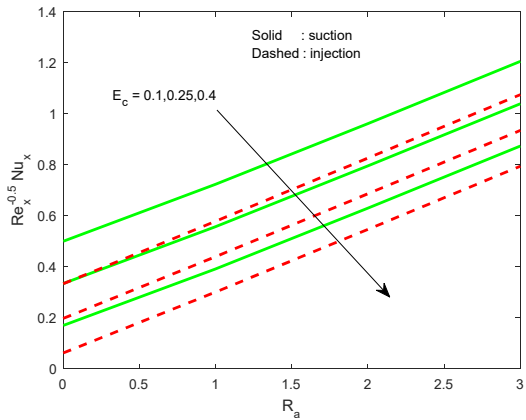


**Figure 12.** Situation in which Nusselt number is impacted by  $E_c$  **Figure 13.** Situation in which Nusselt number is impacted by  $\Lambda$

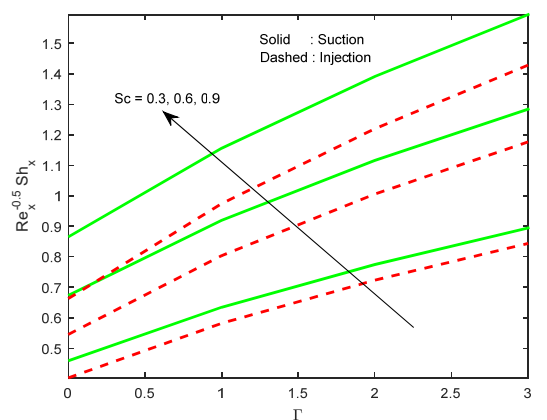
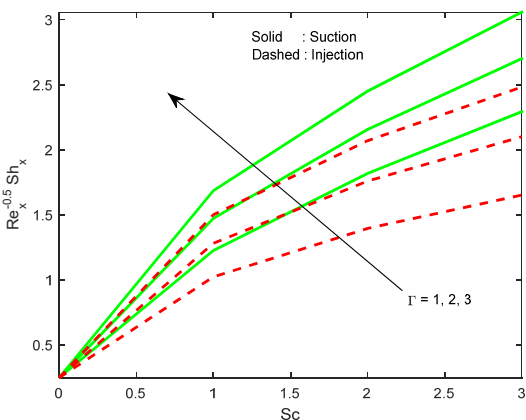


**Figure 14.** Situation in which Sherwood number is impacted by  $\Gamma$  **Figure 15.** Situation in which Sherwood number is impacted by  $Sc$



### 4.5. Bejan number and other profiles

As the Brinkman number rises, indicating a higher ratio of viscous dissipation to thermal conduction, the internal heat generation in the fluid increases. This results in larger temperature gradients and greater irreversibility in the heat transfer processes, leading to increased entropy generation (see Fig. 16).

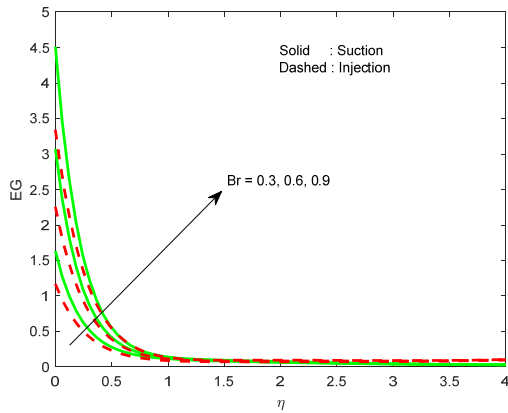


Figure 16. Situation in which entropy generation is impacted by  $Br$

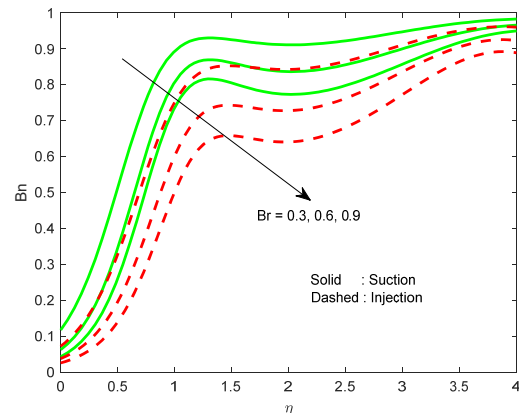


Figure 17. Situation in which Bejan number is impacted by  $Br$

An increase in the Brinkman number highlights the growing significance of viscous dissipation within the fluid, leading to greater irreversibility associated with fluid flow. This shift in the balance of irreversibility reduces the Bejan number, indicating that viscous dissipation becomes the dominant source of entropy generation in the system, overshadowing the irreversibility due to heat transfer (see Fig. 17). From Figs. 18-19, it is clear that the rise in thermal radiation parameter leads to the escalation in both entropy generation and Bejan number.

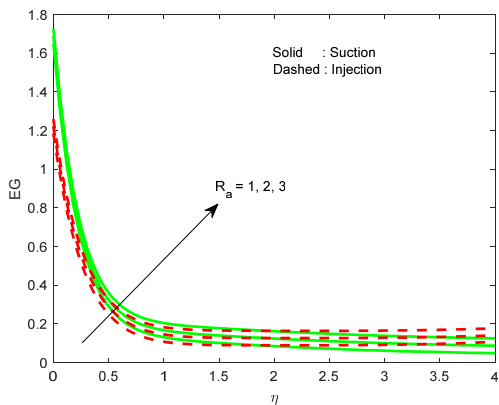


Figure 18. Situation in which entropy generation is impacted by  $R_a$

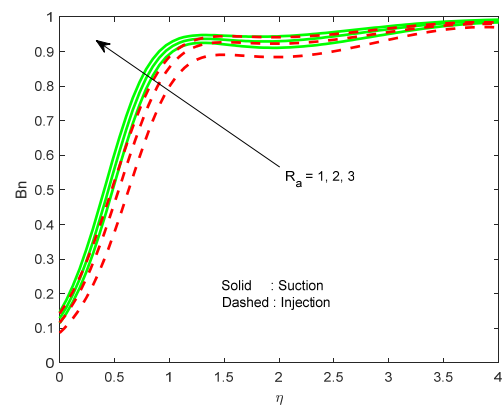


Figure 19. Situation in which Bejan number is impacted by  $R_a$

## 5. CONCLUSIONS

Entropy generation optimization in Ree-Eyring ternary hybrid nanofluid flow across an angled stretched sheet subject to Thompson Troian boundary conditions has been investigated numerically. Careful observations from the numerical results, the following are the main takeaways from this study:

- Ree-Eyring parameter elevates fluid velocity.
- Raise in the slip parameter of velocity leads to the decrement in fluid velocity.
- Eckert number and thermal relaxation parameter exhibited different influences on temperature.
- Concentration profile contracts with bigger chemical reaction parameter.
- Friction factor is bearing a considerable negative connection with  $We$ .
- Sherwood number is bearing a significant progressive correlation with  $Sc, \Gamma$ .
- When  $Br$  enhances, Viscous dissipation's contribution to overall irreversibility becomes increasingly noticeable. So that Bejan number declines.
- Enhanced thermal radiation parameter causes to the escalation in both entropy generation and Bejan number.

### ORCID

- Gadamsetty Revathi, <https://orcid.org/0000-0001-9419-2637>; 
 D. Purnachandra Rao, <https://orcid.org/0000-0002-3128-8137>;  
 S. Ramalingeswara Rao, <https://orcid.org/0000-0002-4445-2637>; 
 K.S. Srinivasa Babu, <https://orcid.org/0000-0002-9292-8214>;  
 T.R.K.D. Vara Prasad, <https://orcid.org/0000-0001-5935-0230>; 
 M. Jayachandra Babu, <https://orcid.org/0000-0001-7645-6301>

## REFERENCES

- [1] M. Sheikholeslami, and H.B. Rokni, "Simulation of nanofluid heat transfer in presence of magnetic field: a review," *International Journal of Heat and Mass Transfer*, **115**, 1203-1233 (2017). <https://doi.org/10.1016/j.ijheatmasstransfer.2017.08.108>
- [2] R.B. Ganvir, P.V. Walke, and V.M. Kriplani, "Heat transfer characteristics in nanofluid—A review," *Renewable and sustainable energy reviews*, **75**, 451-460 (2017). <https://doi.org/10.1016/j.rser.2016.11.010>
- [3] G. Revathi, G. Veeram, M.J. Babu, K.S.S. Babu, and A. Suneel Kumar, "Darcy–Forchheimer flow of power-law (Ostwald-de Waele type) nanofluid over an inclined plate with thermal radiation and activation energy: an irreversibility analysis," *International Journal of Ambient Energy*, **44**(1), 1980–1989 (2023). <https://doi.org/10.1080/01430750.2023.2200434>
- [4] G. Rasool, A. Shafiq, X. Wang, A.J. Chamkha, and A. Wakif, "Numerical treatment of MHD Al<sub>2</sub>O<sub>3</sub>–Cu/engine oil-based nanofluid flow in a Darcy–Forchheimer medium: application of radiative heat and mass transfer laws," *International Journal of Modern Physics B*, **38**(09), 2450129 (2024). <https://doi.org/10.1142/S0217979224501297>
- [5] S. Li, M. Faizan, F. Ali, G. Ramasekhar, T. Muhammad, H.A.E.W. Khalifa, and Z. Ahmad, "Modelling and analysis of heat transfer in MHD stagnation point flow of Maxwell nanofluid over a porous rotating disk," *Alexandria Engineering Journal*, **91**, 237-248 (2024). <https://doi.org/10.1016/j.aej.2024.02.002>
- [6] J.K. Madhukesh, S.O. Paramesh, G.D. Prasanna, B.C. Prasannakumara, M.I. Khan, S. Abdullaev, and G. Rasool, "Impact of magnetized nanoparticle aggregation over a Riga plate with thermal radiation in water-Al<sub>2</sub>O<sub>3</sub> based nanofluid flow," *ZAMM-Journal of Applied Mathematics and Mechanics/Zeitschrift für Angewandte Mathematik und Mechanik*, e202300270 (2024). <https://doi.org/10.1002/zamm.202300270>
- [7] M. Yasir, M. Khan, A.S. Alqahtani, and M.Y. Malik, "Heat generation/absorption effects in thermally radiative mixed convective flow of Zn–TiO<sub>2</sub>/H<sub>2</sub>O hybrid nanofluid," *Case Studies in Thermal Engineering*, **45**, 103000 (2023). <https://doi.org/10.1016/j.csite.2023.103000>
- [8] Y.B. Kho, R. Jusoh, M.Z. Salleh, M.H. Ariff, and N. Zainuddin, "Magnetohydrodynamics flow of Ag-TiO<sub>2</sub> hybrid nanofluid over a permeable wedge with thermal radiation and viscous dissipation," *Journal of Magnetism and Magnetic Materials*, **565**, 170284 (2023). <https://doi.org/10.1016/j.jmmm.2022.170284>
- [9] M. Abbas, N. Khan, M.S. Hashmi, and J. Younis, "Numerically analysis of Marangoni convective flow of hybrid nanofluid over an infinite disk with thermophoresis particle deposition," *Scientific Reports*, **13**(1), 5036 (2023). <https://doi.org/10.1038/s41598-023-32011-x>
- [10] S.A. Khan, M. Imran, H. Waqas, T. Muhammad, S. Yasmin, and A. Alhushaybari, "Numerical analysis of multiple slip effects on CuO/MgO/TiO<sub>2</sub>-water ternary hybrid nanofluid with thermal and exponential space-based heat source," *Tribology International*, **197**, 109778 (2024). <https://doi.org/10.1016/j.triboint.2024.109778>
- [11] A. Mishra, and G. Pathak, "A comparative analysis of MoS<sub>2</sub>-SiO<sub>2</sub>/H<sub>2</sub>O hybrid nanofluid and MoS<sub>2</sub>-SiO<sub>2</sub>-GO/H<sub>2</sub>O ternary hybrid nanofluid over an inclined cylinder with heat generation/absorption," *Numerical Heat Transfer, Part A: Applications*, **85**(16), 2724-2753 (2024). <https://doi.org/10.1080/10407782.2023.2228483>
- [12] Najafpour, K. Hosseinzadeh, J.R. Kermani, A.A. Ranjbar, and D.D. Ganji, "Numerical study on the impact of geometrical parameters and employing ternary hybrid nanofluid on the hydrothermal performance of mini-channel heat sink," *Journal of Molecular Liquids*, **393**, 123616 (2024). <https://doi.org/10.1016/j.molliq.2023.123616>
- [13] U. Farooq, A. Bibi, J.N. Abbasi, A. Jan, and M. Hussain, "Nonsimilar mixed convection analysis of ternary hybrid nanofluid flow near stagnation point over vertical Riga plate," *Multidiscipline Modeling in Materials and Structures*, **20**(2), 261-278 (2024). <https://doi.org/10.1108/MMMS-09-2023-0301>
- [14] M. Mahboobtosi, K. Hosseinzadeh, and D.D. Ganji, "Investigating the convective flow of ternary hybrid nanofluids and single nanofluids around a stretched cylinder: Parameter analysis and performance enhancement," *International Journal of Thermofluids*, **23**, 100752 (2024). <https://doi.org/10.1016/j.ijft.2024.100752>
- [15] D. Mohanty, G. Mahanta, and S. Shaw, "Irreversibility and thermal performance of nonlinear radiative cross-ternary hybrid nanofluid flow about a stretching cylinder with industrial applications," *Powder Technology*, **433**, 119255 (2024). <https://doi.org/10.1016/j.powtec.2023.119255>
- [16] T. Hayat, S.A. Khan, M.I. Khan, S. Momani, and A. Alsaedi, "Cattaneo-Christov (CC) heat flux model for nanomaterial stagnation point flow of Oldroyd-B fluid," *Computer methods and programs in biomedicine*, **187**, 105247 (2020). <https://doi.org/10.1016/j.cmpb.2019.105247>
- [17] S. Ahmad, S. Nadeem, N. Muhammad, and M.N. Khan, "Cattaneo–Christov heat flux model for stagnation point flow of micropolar nanofluid toward a nonlinear stretching surface with slip effects," *Journal of Thermal Analysis and Calorimetry*, 1-13, (2020). <https://doi.org/10.1007/s10973-020-09504-2>
- [18] W. Ibrahim, and G. Gadisa, "Finite element solution of nonlinear convective flow of Oldroyd-B fluid with Cattaneo–Christov heat flux model over nonlinear stretching sheet with heat generation or absorption," *Propulsion and Power Research*, **9**(3), 304-315 (2020). <https://doi.org/10.1016/j.jprr.2020.07.001>
- [19] M.G. Reddy, M.S. Rani, K.G. Kumar, B.C. Prasannakumar, and H.J. Lokesh, "Hybrid dusty fluid flow through a Cattaneo–Christov heat flux model," *Physica A: Statistical Mechanics and its Applications*, **551**, 123975 (2020). <https://doi.org/10.1016/j.physa.2019.123975>
- [20] B.J. Gireesha, B.M. Shankaralingappa, B.C. Prasannakumar, and B. Nagaraja, "MHD flow and melting heat transfer of dusty Casson fluid over a stretching sheet with Cattaneo–Christov heat flux model," *International Journal of Ambient Energy*, **43**(1), 2931-2939 (2020). <https://doi.org/10.1080/01430750.2020.1785938>
- [21] A.R.A. Naqvi, A. Haider, D. Hussain, and S. Hussain, "Finite Element Study of MHD Impacts on the Rotating Flow of Casson Nanofluid with the Double Diffusion Cattaneo–Christov Heat Flux Model," *Mathematics*, **8**(9), 1555 (2020). <https://doi.org/10.3390/math8091555>
- [22] Tassaddiq, "Impact of Cattaneo-Christov heat flux model on MHD hybrid nano-micropolar fluid flow and heat transfer with viscous and joule dissipation effects," *Scientific Reports*, **11**(1), 1-14 (2021). <https://doi.org/10.1038/s41598-020-77419-x>
- [23] S. Jakeer, P.B. Reddy, A.M. Rashad, and H.A. Nabwey, "Impact of heated obstacle position on magneto-hybrid nanofluid flow in a lid-driven porous cavity with Cattaneo-Christov heat flux pattern," *Alexandria Engineering Journal*, **60**(1), 821-835 (2021). <https://doi.org/10.1016/j.aej.2020.10.011>

- [24] Mahesh, S.V.K. Varma, C.S.K. Raju, M.J. Babu, I.L. Animasaun, and N.A. Shah, "Significance of Reynolds number, lower and upper rotating disks on the dynamics of water conveying graphene and silver nanoparticles between rotating disks," *Physica Scripta*, **96**(4), 045218 (2021). <https://doi.org/10.1088/1402-4896/abe2d3>
- [25] Ali, S. Hussain, Y. Nie, A.K. Hussein, and D. Habib, "Finite element investigation of Dufour and Soret impacts on MHD rotating flow of Oldroyd-B nanofluid over a stretching sheet with double diffusion Cattaneo Christov heat flux model," *Powder Technology*, **377**, 439-452 (2021). <https://doi.org/10.1016/j.powtec.2020.09.008>
- [26] H. Sharif, M.A. Khadimallah, M.N. Naeem, M. Hussain, S. Hussain, and A. Tounsi, "Flow of MHD Powell-Eyring nanofluid: Heat absorption and Cattaneo-Christov heat flux model," *Advances in nano research*, **10**(3), 221-234 (2021). <https://doi.org/10.12989/anr.2021.10.3.221>
- [27] S. Ahmad, S. Nadeem, and M.N. Khan, "Mixed convection hybridized micropolar nanofluid with triple stratification and Cattaneo-Christov heat flux model," *Physica Scripta*, **96**, 075205 (2021). <https://doi.org/10.1088/1402-4896/abf615>
- [28] A. Jafarimoghaddam, M. Turkyilmazoglu, and I. Pop, "Threshold for the generalized Non-Fourier heat flux model: Universal closed form analytic solution," *International Communications in Heat and Mass Transfer*, **123**, 105204 (2021). <https://doi.org/10.1016/j.icheatmasstransfer.2021.105204>
- [29] Z. Hussain, A. Hussain, M.S. Anwar, and M. Farooq, "Analysis of Cattaneo-Christov heat flux in Jeffery fluid flow with heat source over a stretching cylinder," *Journal of Thermal Analysis and Calorimetry*, **147**, 3391-3402 (2021). <https://doi.org/10.1007/s10973-021-10573-0>
- [30] A. Bhattacharyya, G.S. Seth, et al., "Simulation of Cattaneo-Christov heat flux on the flow of single and multi-walled carbon nanotubes between two stretchable coaxial rotating disks," *Journal of Thermal Analysis and Calorimetry*, **139**, 1655-1670 (2020). <https://doi.org/10.1007/s10973-019-08644-4>
- [31] S. Khattak, M. Ahmed, M.N. Abrar, S. Uddin, M. Sagheer, and M. Farooq Javeed, "Numerical simulation of Cattaneo-Christov heat flux model in a porous media past a stretching sheet," *Waves in Random and Complex Media*, 1-20 (2022). <https://doi.org/10.1080/17455030.2022.2030503>
- [32] R.P. Gowda, R.N. Kumar, R. Kumar, and B.C. Prasannakumara "Three-dimensional coupled flow and heat transfer in non-Newtonian magnetic nanofluid: An application of Cattaneo-Christov heat flux model," *Journal of Magnetism and Magnetic Materials*, **567**, 170329 (2023). <https://doi.org/10.1016/j.jmmm.2022.170329>
- [33] M.I.U. Rehman, H. Chen, A. Hamid, and K. Guedri, "Analysis of Cattaneo-Christov heat flux and thermal radiation on Darcy-Forchheimer flow of Reiner-Philippoff fluid," *International Journal of Modern Physics B*, **38**(03), 2450046 (2024). <https://doi.org/10.1142/S0217979224500462>
- [34] S.A. Khan, Y. Nie, and B. Ali, "Multiple slip effects on MHD unsteady viscoelastic nano-fluid flow over a permeable stretching sheet with radiation using the finite element method," *SN Applied Sciences*, **2**(66), (2020). <https://doi.org/10.1007/s42452-019-1831-3>
- [35] G. Rasool, T. Zhang, A.J. Chamkha, A. Shafiq, I. Tlili, and G. Shahzadi, "Entropy generation and consequences of binary chemical reaction on MHD Darcy-Forchheimer Williamson nanofluid flow over non-linearly stretching surface," *Entropy*, **22**(1), 18 (2020). <https://doi.org/10.3390/e22010018>
- [36] T. Abbas, S. Rehman, R.A. Shah, M. Idrees, and M. Qayyum, "Analysis of MHD Carreau fluid flow over a stretching permeable sheet with variable viscosity and thermal conductivity," *Physica A: Statistical Mechanics and its Applications*, **551**, 124225 (2020). <https://doi.org/10.1016/j.physa.2020.124225>
- [37] A. Yasmin, K. Ali, and M. Ashraf, "Study of heat and mass transfer in MHD flow of micropolar fluid over a curved stretching sheet," *Scientific reports*, **10**(1), 1-11 (2020). <https://doi.org/10.1038/s41598-020-61439-8>
- [38] S.S. Giri, K. Das, and P.K. Kundu, "Homogeneous-heterogeneous reaction mechanism on MHD carbon nanotube flow over a stretching cylinder with prescribed heat flux using differential transform method," *Journal of Computational Design and Engineering*, **7**(3), 337-351 (2020). <https://doi.org/10.1093/jcde/qwaa028>
- [39] M. Gayatri, K.J. Reddy, and M.J. Babu, "Slip flow of Carreau fluid over a slendering stretching sheet with viscous dissipation and Joule heating," *SN Applied Sciences*, **2**(3), 1-11 (2020). <https://doi.org/10.1007/s42452-020-2262-x>
- [40] M.A. Kumar, Y.D. Reddy, V.S. Rao, and B.S. Goud, "Thermal radiation impact on MHD heat transfer natural convective nano fluid flow over an impulsively started vertical plate," *Case Studies in Thermal Engineering*, **24**, 100826 (2021). <https://doi.org/10.1016/j.csite.2020.100826>
- [41] N.S. Elgazery, "CPSM Simulation of the Variable Properties' Role in MHD Non-Newtonian Micropolar Nanofluid Flow Over a Stretching Porous Sheet (Flow Filtration)," *Arab Journal for Science and Engineering*, **46**, 7661-7680 (2021). <https://doi.org/10.1007/s13369-021-05489-8>
- [42] P. Pavar, L. Harikrishna, and M.S. Reddy, "Heat transfer over a stretching porous surface on a steady MHD fluid flow," *International Journal of Ambient Energy*, **43**(1), 4398-4405 (2022). <https://doi.org/10.1080/01430750.2020.1848915>
- [43] S.M. Abo-Dahab, M.A. Abdelhafez, F. Mebarek-Oudina et al., "MHD Casson nanofluid flow over nonlinearly heated porous medium in presence of extending surface effect with suction/injection," *Indian Journal Physics*, **95**, 2703-2717 (2021). <https://doi.org/10.1007/s12648-020-01923-z>
- [44] A.M. Megahed, M.G. Reddy, and W. Abbas, "Modeling of MHD fluid flow over an unsteady stretching sheet with thermal radiation, variable fluid properties and heat flux," *Mathematics and Computers in Simulation*, **185**, 583-593 (2021). <https://doi.org/10.1016/j.matcom.2021.01.011>
- [45] Nagaraja, and B.J. Gireesha, "Exponential space-dependent heat generation impact on MHD convective flow of Casson fluid over a curved stretching sheet with chemical reaction," *Journal of Thermal Analysis and Calorimetry*, **143**, 4071-4079 (2021). <https://doi.org/10.1007/s10973-020-09360-0>
- [46] A. Hussain, and M.Y. Malik, "MHD nanofluid flow over stretching cylinder with convective boundary conditions and Nield conditions in the presence of gyrotactic swimming microorganism: A biomathematical model," *International Communications in Heat and Mass Transfer*, **126**, 105425 (2021). <https://doi.org/10.1016/j.icheatmasstransfer.2021.105425>
- [47] K.S.S. Babu, A. Parandhama, and R.B. Vijaya, "Non-linear MHD convective flow of Carreau nanofluid over an exponentially stretching surface with activation energy and viscous dissipation," *SN Applied Sciences*, **3**(3), 382 (2021). <https://doi.org/10.1007/s42452-021-04339-4>

- [48] H.U. Rasheed, S. Islam, Z.W. Khan, J. Khan, and T. Abbas, "Numerical modeling of unsteady MHD flow of Casson fluid in a vertical surface with chemical reaction and Hall current", *Advances in Mechanical Engineering*, **14**(3), (2022). <https://doi.org/10.1177/16878132221085429>
- [49] K.S.S. Babu, A. Parandhama, and R.B. Vijaya, "Significance of heat source/sink on the radiative flow of Cross nanofluid across an exponentially stretching surface towards a stagnation point with chemical reaction," *Heat Transfer*, **51**(4), 2885-2904 (2022). <https://doi.org/10.1002/htj.22428>
- [50] B. Jalili, A.M. Ganji, A. Shateri, P. Jalili, and D.D. Ganji, "Thermal analysis of Non-Newtonian visco-inelastic fluid MHD flow between rotating disks," *Case Studies in Thermal Engineering*, **49**, 103333 (2023). <https://doi.org/10.1016/j.csite.2023.103333>
- [51] G. Revathi, V.S. Sajja, M.J. Babu, K.S.S. Babu, A.S. Kumar, C.S.K. Raju, and S.J. Yook, "Multiple linear regression analysis on the flow of ternary hybrid nanofluid by a quadratically radiated stretching surface with and second order slip," *Waves in Random and Complex Media*, 1-18 (2023). <https://doi.org/10.1080/17455030.2023.2181645>
- [52] K. Ahmed, T. Akbar, I. Ahmed, T. Muhammad, and M. Amjad, "Mixed convective MHD flow of Williamson fluid over a nonlinear stretching curved surface with variable thermal conductivity and activation energy," *Numerical Heat Transfer, Part A: Applications*, **85**(6), 942-957 (2024). <https://doi.org/10.1080/10407782.2023.2194689>
- [53] S. Ahmad, and S. Nadeem, "Flow analysis by Cattaneo–Christov heat flux in the presence of Thomson and Troian slip condition," *Applied Nanoscience*, **10**(12), 4673-4687 (2020). <https://doi.org/10.1007/s13204-020-01267-4>
- [54] K. Rafique, M.I. Anwar, M. Misiran, I. Khan, and E.S.M. Sherif, "The implicit Keller Box scheme for combined heat and mass transfer of Brinkman-type micropolar nanofluid with Brownian motion and thermophoretic effect over an inclined surface," *Applied Sciences*, **10**(1), 280 (2019). <https://doi.org/10.3390/app10010280>
- [55] S.P. Anjali Devi, and P. Suriyakumar, "Numerical investigation of mixed convective hydromagnetic nonlinear nanofluid flow past an inclined plate," *AIP Conference Proceedings*, **1557**(1), 281-285 (2013). <https://doi.org/10.1063/1.4823920>

### ОПТИМІЗАЦІЯ ГЕНЕРАЦІЇ ЕНТРОПІЇ В ПОТРІЙНІЙ ГІБРИДНІЙ НАНОРІДИНІ РЕ-ЕЙРІНГА ПО ПРУЖНІЙ ПОВЕРХНІ З НЕ ФУР'Є ТЕПЛОВИМ ПОТОКОМ

Гадамсетгі Реваті<sup>a</sup>, Д. Пурначандра Рао<sup>b</sup>, С. Рамалінгесвара Рао<sup>c</sup>, К.С. Шрініваса Бабу<sup>c</sup>, Т.Р.К.Д. Вара Прасад<sup>c</sup>, М. Джаячандра Бабу<sup>d</sup>

<sup>a</sup>Департамент математики, Інститут інженерії та технології Гокараджу Рангараджу, Бачупаллі, Хайдарабад, Індія

<sup>b</sup>Факультет математики, Інженерний коледж Матрусі, Саїдабад, Хайдарабад, Телангана, Індія

<sup>c</sup>Департамент ЕМ&Н, S.R.K.R. Інженерний коледж, Бхімаварам, Андхра-Прадеш, Індія

<sup>d</sup>Факультет математики Державного коледжу, Раджампета, район Аннамайя, Андхра-Прадеш, Індія

Значення потрійного гібридного потоку нанорідини Ree-Eyring полягає в його потенційному застосуванні в різних областях. Завдяки введенню трьох різних типів наночастинок в базову рідину за допомогою моделі Рі-Айрінга ця інноваційна рідина забезпечує покращену теплопровідність, ефективність теплопередачі та реологічні властивості. Ці характеристики особливо цінні в таких галузях, як охолодження електроніки, сонячні енергетичні системи та теплообмінники, де ефективне керування теплом має вирішальне значення. Крім того, унікальна реологічна поведінка нанофлюїдів Рі-Айрінга може забезпечити переваги в таких процесах, як свердління, змащення та доставка ліків. У граничних умовах Томпсона-Трояна це дослідження має на меті теоретично проаналізувати двовимірний радіаційний потік потрійної гібридної нанорідини Рі-Айрінга над кутовим листом з тепловим потоком Каттанео-Крістова та параметрами хімічної реакції вищого порядку. Щоб виразити їх як звичайні диференціальні рівняння (ОДУ), рівняння, керовані потоком, зазнають відповідних перетворень подібності. Наступна система вирішується за допомогою підходу  $bvp4c$ . Основний висновок цього дослідження полягає в тому, що параметр теплової релаксації зменшує ширину температурного профілю, а швидкість рідини мінімізується шляхом регулювання параметра ковзання. Профіль концентрації мінімізується параметром хімічної реакції, а параметр рідини Рі-Айрінга зростає з тим самим (швидкістю рідини). Крім того, ми виявили, що коефіцієнт шкірного тертя сильно негативно корелює з параметром рідини Рі-Айрінга, позитивно з параметром (термічної) релаксації та значно позитивно корелює з хімічною реакцією через число Нуссельта. Коли число Брінкмана збільшується, число Бежана падає. Крім того, підвищення параметра теплового випромінювання призводить до ескалації як генерації ентропії, так і числа Бежана. Ми помітили гідну згоду, коли перевіряли результати цього розслідування з попередніми наслідками.

**Ключові слова:** в'язка дисипація; теплове випромінювання; МГД; не Фур'є тепловий потік; нанофлюїд